Preprints of the 21st IFAC World Congress (Virtual)
Berlin, Germany, July 12-17, 2020

An efficient model-error model update strategy for multi-stage NMPC with model-error model

Sakthi Thangavel [*] **Sebastian Engell** [*]

[*] *Process Dynamics and Operations Group, Technische Universität Dortmund, Emil-Figge-Straße 70, 44227 Dortmund, Germany (e-mail: sakthi.thangavel@tu-dortmund.de)*

Abstract: Multi-stage NMPC with model-error model (MS-MEM) handles structural plant-model mismatch present in the nominal model of the plant in a non-conservative fashion. A model-error model (MEM) that consists of a stable linear time-invariant dynamics and a static time-variant nonlinear mapping is built using the past data such that it captures the unmodeled dynamics of the plant. The scenario tree is built for the nominal and for the extreme realizations of the plant obtained using the nominal model and the model-error model, and a multi-stage decision problem is formulated. In this paper, we propose an efficient strategy to update the model-error model present in the MS-MEM approach if new measurements invalidate the model-error model. The advantages of the proposed scheme over the previous approach where only the gain of the linear model is updated are demonstrated for a continuous stirred tank reactor (CSTR) benchmark example.

Keywords: Adaptive control, Model-error model, Multi-stage NMPC, Nonlinear model predictive control, Process control, Robust control

1. INTRODUCTION

Model predictive control (MPC) is broadly used in the process industries because of its ability to handle MIMO systems and constraints. The performance of such controllers may deteriorate and constraint violations may occur in the presence of plant-model mismatch which can be avoided by adopting robust MPC strategies. The most prominent ones are the min-max MPC (Campo and Morari, 1987), the tube-based MPC (Mayne et al., 2005), and the multi-stage MPC (Lucia et al., 2012, 2013).

Min-max MPC solves the MPC optimization problem for the worst-case realization of the uncertainty (Campo and Morari, 1987; Scokaert and Mayne, 1998). Tube-based MPC uses two controllers, a primary controller and an ancillary controller (Mayne et al., 2005). The primary controller computes an optimal control trajectory using the nominal model of the plant and the ancillary controller tracks it. Multi-stage MPC models a decision problem under uncertainty (which can be unknown disturbance or parametric uncertainty) by a tree of discrete scenarios (Lucia et al., 2013). Multi-stage MPC explicitly takes into account the presence of future feedback information in the computation of its control moves and therefore, it is less conservative than other robust MPC approaches. Several variants of the multi-stage NMPC exist in literature (Thangavel et al., 2018a,b, 2020). However, dealing with the presence of structural plant-model mismatch still remains an open area of research (Mayne, 2014).

Falugi and Mayne (2014) extended the tube-based NMPC method to handle structural plant-model mismatch. The unstructured uncertainty is modeled as an additive disturbance by imposing additional hard constraints on the plant output. Subramanian et al. (2015) modeled the presence of structural plant-model mismatch as a time-varying additive bounded disturbance and handled it in a multi-stage NMPC framework. This, however, led to a significant loss in performance compared to the case without structural uncertainty. (Thangavel et al., 2018c) considered an additive model-error model (MEM) which consists of a linear model followed by an unknown nonlinear static operator with bounded gain to capture the unmodeled dynamics of the plant. The key idea here is that the model error is different for different frequencies and not the same upper bound for the induced norm of the MEM is assumed at all frequencies, which strongly reduces the conservativeness of the MEM. The MEM is built using the data collected from the previous plant operations and the scenario tree of multistage NMPC is built using the combined nominal model and the model-error model. This results in a significant improvement in the performance when compared to the case where the structural plant-model mismatch is modeled as an additive disturbance with bounded variation (Thangavel et al., 2018c).

The robustness of multi-stage NMPC with model-error model (MS-MEM) depends on the accuracy of the model-error model that is considered. The MEM is valid only for the data that was used to build it. In order to take into account that the structural uncertainty may be larger than observed in the past, a tuning parameter was introduced in MS-MEM approach to over-approximate the uncertainty region and in addition, the validity of the model-error model is checked whenever a new measurement information from the plant becomes available (Poolla et al., 1994). If the MEM is invalidated by the observed measurement, the gain of the linear model that is present in the MEM is updated such that the updated MEM describes all the observed measurements. However, this is done uniformly for all frequencies and therefore over-approximates the model uncertainty and results in a performance loss. The performance can be improved by recomputing the model-error model using all the available measurements (both online data - from the current plant operation and offline data - from previous plant runs) whenever the model-error model is invalidated. However, this will result in an optimization problem at each MPC iteration which may not be feasible to solve in real-time.

In this paper, we propose to solve a simplified optimization problem to adapt the MEM which approximates the information provided by the offline data and uses only the online data to build the MEM. The proposed approach guarantees that the uncertainty region which is described by the updated model-error model contains the uncertainty region described by the model-error model built using the offline data.

2. MODEL-ERROR MODEL (MEM)

The nonlinear dynamics of the plant is given by

$$\boldsymbol{z}_{k+1} = \boldsymbol{h}(\boldsymbol{z}_k, \boldsymbol{u}_k), \tag{1}$$

where $\boldsymbol{h} : \mathbb{R}^{n_z} \times \mathbb{R}^{n_u} \to \mathbb{R}^{n_z}$ is an unknown smooth nonlinear function, $\boldsymbol{z}_k \in \mathbb{R}^{n_z}$ and $\boldsymbol{u}_k \in \mathbb{R}^{n_u}$ represent the true plant state and control input, n_z and n_u give the number of plant states and control inputs. The nominal model of the plant is given by

$$\boldsymbol{x}_{k+1} = \boldsymbol{f}(\boldsymbol{x}_k, \boldsymbol{u}_k), \tag{2}$$

where $\boldsymbol{f} : \mathbb{R}^{n_x} \times \mathbb{R}^{n_u} \to \mathbb{R}^{n_x}$ is a known smooth nonlinear function, $\boldsymbol{x}_k \in \mathbb{R}^{n_x}$ represents the state of the model equation and n_x is the number of modeled states. We assume that only the model states are measured and no further information from the plant is available (i.e. about the hidden states or dynamics). In this paper, we refer to all the data stored during the past plant operations as offline data and the data collected during the current plant run as online data.

The error between the true dynamics of the plant and the nominal model reinitialized at the plant measurement is given by

$$\boldsymbol{e}_{k+1} = \mathbb{P}(\boldsymbol{h}(\boldsymbol{z}_k, \boldsymbol{u}_k)) - \boldsymbol{f}(\mathbb{P}(\boldsymbol{z}_k), \boldsymbol{u}_k), \tag{3}$$

where $\mathbb{P} : \mathbb{R}^{n_z} \to \mathbb{R}^{n_x}$ is a projection operator which projects the plant states onto the model states and $\boldsymbol{e}_k$ represents the discrepancy between the nominal model predictions and the projected plant measurements. An uncertainty region which encloses the unmodeled dynamics of the plant can be obtained using a linear stable dynamic model and an unknown (possible nonlinear and time varying) static mapping ($\boldsymbol{\Delta}_k$) with bounded gain (Poolla et al., 1994; Ljung, 2001) as shown in Fig. 1. The chosen model-error model (MEM) structure can be written as

$$\hat{\boldsymbol{e}}_{k+1} = \boldsymbol{A^e}\hat{\boldsymbol{e}}_k + \boldsymbol{B^e}\boldsymbol{u}_k, \tag{4a}$$

$$\boldsymbol{\Delta}_{k+1}(\hat{\boldsymbol{e}}_{k+1}) := \left[\delta^1_{k+1}(\hat{e}_{k+1,[1]}), \cdots, \delta^{n_x}_{k+1}(\hat{e}_{k+1,[n_x]})\right]^T, \tag{4b}$$

$$\left\|\delta^s_{k+1}\right\|_{i\infty} \leq 1, \quad \forall s \in \mathcal{I}_1 := \{1, \cdots, n_x\}, \tag{4c}$$

$$\boldsymbol{e}_{k+1} = \boldsymbol{\Delta}_{k+1}(\hat{\boldsymbol{e}}_{k+1}), \tag{4d}$$

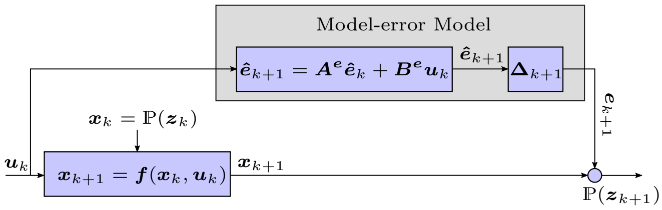

Fig. 1. Model-error model (MEM) structure.

where $\boldsymbol{A^e} \in \mathbb{R}^{n_x \times n_x}, \boldsymbol{B^e} \in \mathbb{R}^{n_x \times n_u}$ describe the dynamics of the state of the linear model ($\hat{\boldsymbol{e}}_k \in \mathbb{R}^{n_x}$) in the model-error model. $\hat{e}_{k,[s]}$ represents the s^{th} element of the vector $\hat{\boldsymbol{e}}_k$. $\boldsymbol{\Delta}_k(\cdot)$ is defined by n_x unknown nonlinear operators δ^s_k, where δ^s_k represents an unknown static nonlinear mapping corresponding to state s and $\|\cdot\|_{i\infty}$ denotes the induced infinity norm of the function. The observed discrepancy between the projected plant measurement and the predicted modeled state reinitialized at the projected plant measurements is described by the model-error model (4).

The model-error model can be obtained from the past observations (offline data) by solving an optimization problem (5), if the plant has been sufficiently excited:

$$\min_{\boldsymbol{A^e_0}, \boldsymbol{B^e_0}, \boldsymbol{D}_{k+1}} \frac{1}{N_m} \sum_{k=0}^{N_m-1} \hat{\boldsymbol{e}}^T_{k+1}\boldsymbol{Q}\hat{\boldsymbol{e}}_{k+1}, \tag{5a}$$

subject to

$$\hat{\boldsymbol{e}}_{k+1} = \boldsymbol{A^e_0}\hat{\boldsymbol{e}}_k + \boldsymbol{B^e_0}\boldsymbol{u}_k, \qquad \forall k \in \mathcal{I}_2, \tag{5b}$$

$$\hat{\boldsymbol{e}}_0 = \mathbb{P}(\boldsymbol{z}_0) - \boldsymbol{x}_0, \quad |\text{eig}(\boldsymbol{A^e_0})| \leq 1, \tag{5c}$$

$$\boldsymbol{D}_{k+1} = \text{diag}([d^1_{k+1}, \cdots, d^{n_x}_{k+1}]), \qquad \forall k \in \mathcal{I}_2, \tag{5d}$$

$$\boldsymbol{e}_{k+1} = \boldsymbol{D}_{k+1}\hat{\boldsymbol{e}}_{k+1}, \qquad k \in \mathcal{I}_2, \tag{5e}$$

$$-1 \leq d^s_{k+1} \leq 1, \qquad \forall s \in \mathcal{I}_1, k \in \mathcal{I}_2, \tag{5f}$$

where $\mathcal{I}_2 := \{0, \cdots, N_m - 1\}$ denotes the indices of the measurements that are used to build the model-error model, N_m is the number of measurements and the diagonal matrix $\boldsymbol{Q} \in \mathbb{R}^{n_x \times n_x}$ is a weighting matrix. $\boldsymbol{A^e_0} \in \mathbb{R}^{n_x \times n_x}, \boldsymbol{B^e_0} \in \mathbb{R}^{n_x \times n_u}$ describe the dynamics of the linear model and $\boldsymbol{D}_k \in \mathbb{R}^{n_x \times n_x}$ denotes the gains of the unknown nonlinear operator $\boldsymbol{\Delta}_k$ obtained using the offline data. The objective function (5a) is chosen to minimize the volume of the uncertainty region around the nominal model. Constraint (5c) enforces stable linear dynamics of the model-error model, where eig$(\cdot)$ gives the eigenvalues of the matrix. Constraints (5e) and (5f) ensure that the uncertainty region described by the model-error model and the static gain-bounded unknown mapping s.t. $\|\delta^s_k\|_{i\infty} \leq 1$ encloses the observed plant-model mismatch. The constraints (5c) and (5e) result in a non-convex optimization problem and can be replaced by a set of linear constraints (6) if the input is one-sided (i.e. there is no change in the sign of the control input), and the structure of $\boldsymbol{A^e}$ is restricted to a diagonal matrix.

$$-\hat{\boldsymbol{e}}_{k+1} \leq \boldsymbol{e}_{k+1} \leq \hat{\boldsymbol{e}}_{k+1}, \qquad \forall k \in \mathcal{I}_2, \tag{6a}$$

$$\hat{\boldsymbol{e}}_0 = \mathbb{P}(\boldsymbol{z}_0) - \boldsymbol{x}_0, \quad -1 \leq A^e_{0,[s,s]} \leq 1, \quad \forall s \in \mathcal{I}_1. \tag{6b}$$

where $A^e_{0,[s,s]}$ represents s^{th} row and column of the matrix $\boldsymbol{A^e_0}$. In the presence of a bounded measurement error, the true projected plant state is not known but a range which encloses it can be obtained using the observed plant measurement corrupted by measurement noise ($\boldsymbol{x^m_k}$), and the measurement error bound ($\boldsymbol{\sigma}_k$). $\boldsymbol{e}_{k+1}$ is given as

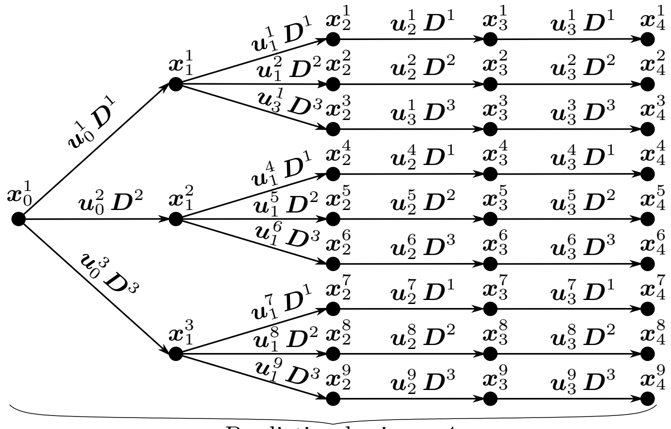

Fig. 2. Scenario tree of the multi-stage NMPC with MEM.

$$\boldsymbol{e}_{k+1} = \boldsymbol{x}^{\boldsymbol{m}}_{k+1} - \boldsymbol{f}(\tilde{\boldsymbol{x}}_k, \boldsymbol{u}_k), \tag{7a}$$

$$\tilde{\boldsymbol{x}}_k = \arg \max_{\boldsymbol{x}^{\boldsymbol{m}}_k - \boldsymbol{\sigma}_k \leq \tilde{\boldsymbol{x}}_k \leq \boldsymbol{x}^{\boldsymbol{m}}_k + \boldsymbol{\sigma}_k} |\boldsymbol{x}^{\boldsymbol{m}}_{k+1} - \boldsymbol{f}(\tilde{\boldsymbol{x}}_k, \boldsymbol{u}_k)|, \tag{7b}$$

and (6a) is replaced by

$$-\hat{\boldsymbol{e}}_{k+1} \leq \boldsymbol{e}_{k+1} \pm \boldsymbol{\sigma}_{k+1} \leq \hat{\boldsymbol{e}}_{k+1}, \quad \forall k \in \mathcal{I}_2, \tag{8}$$

such that the nominal model along with the model-error model encloses the projected true plant state. In the absence of a sufficient level of excitation in the offline data, probing inputs should be applied to plant to capture the unmodeled dynamics of the plant. An overview on the generation of excitation signals for system identification is given in Schoukens et al. (2016).

3. MULTI-STAGE NMPC WITH MEM (MS-MEM)

Multi-stage NMPC describes the evolution of the state trajectories for different realizations of the uncertainty in the form of a tree of discrete scenarios as shown in Fig. 2. Each branch in the scenario tree corresponds to a particular realization of the uncertainty. Multi-stage NMPC considers the presence of measurement information in the future, i.e. the information that the system is at a particular node of the tree and the future control inputs are adapted accordingly. This results in a better performance when compared to open-loop robust NMPC approaches (Lucia et al., 2012, 2013).

Multi-stage NMPC with model-error model (MS-MEM) considers the nominal model of the plant along with the MEM at each node in the scenario tree to handle structural plant-model mismatch. The model is given as

$$\begin{bmatrix} \boldsymbol{x}^j_{k+1} \\ \hat{\boldsymbol{e}}^j_{k+1} \end{bmatrix} = \begin{bmatrix} \boldsymbol{f}(\boldsymbol{x}^{p(j)}_k, \boldsymbol{u}^j_k) \\ \boldsymbol{0}^{n_x} \end{bmatrix} + \begin{bmatrix} \boldsymbol{D}^{r(j)} \boldsymbol{A}^{\boldsymbol{e}} \\ \boldsymbol{A}^{\boldsymbol{e}} \end{bmatrix} \begin{bmatrix} \boldsymbol{x}^{p(j)}_k \\ \hat{\boldsymbol{e}}^{p(j)}_k \end{bmatrix} + \begin{bmatrix} \boldsymbol{D}^{r(j)} \boldsymbol{B}^{\boldsymbol{e}} \\ \boldsymbol{B}^{\boldsymbol{e}} \end{bmatrix} \boldsymbol{u}^j_k. \tag{9}$$

The state prediction ($\boldsymbol{x}^j_{k+1}$) at stage $k+1$ and position j in the scenario tree is given by the parent state ($\boldsymbol{x}^{p(j)}_k$), control input ($\boldsymbol{u}^j_k$), parent model-error model state ($\hat{\boldsymbol{e}}^{p(j)}_k$) and the realization of the gain $\boldsymbol{D}^{r(j)}$ which is a diagonal matrix of dimension n_x. By the construction of the model-error model, the extreme values of the diagonal elements of $\boldsymbol{D}^{r(j)}$ are ± 1 (i.e. the maximum absolute values of d^s_k are 1). This is however valid only for the data that was used to build the MEM. The possible variations in the future model uncertainty (due to unaccounted data) as well as the inaccuracies of the MEM can be counteracted by introducing the tuning parameter $\boldsymbol{\Lambda}$ (called the robust factor). The robust factor is a vector of dimension n_x with $\Lambda_{[s]} \geq 1$, where s denotes the index of the modeled state. The robust factor is chosen based on the accuracy of the model-error model. In the presence of a good MEM (which can be obtained if sufficiently many plant measurements in the optimal operating region of the plant are available), $\Lambda_{[s]}$ is chosen as 1 and in the presence of a poor MEM, $\Lambda_{[s]}$ is chosen larger than 1. The elements $D^{r(j)}_{[s,s]}$ can take values in $\{-\Lambda_{[s]}, 0, \Lambda_{[s]}\}$. If $D^{r(j)}_{[s,s]} = 0$, the nominal model is considered in the predictions, if $D^{r(j)}_{[s,s]} = -\Lambda_{[s]}$ or $\Lambda_{[s]}$, the nominal model along with the MEM is used to predict the extreme realizations of the plant dynamics. This results in 3^{n_x} branches that are considered at each node in the scenario tree. This results in a rapid growth of the scenario tree along the prediction horizon and can be controlled by stopping the branching under the assumption that the uncertainty remains constant after a certain stage known as the robust horizon (N_r).

The optimization problem which is solved at each sampling instance is given by

$$\min_{\boldsymbol{x}^j_k, \hat{\boldsymbol{e}}^j_k, \boldsymbol{u}^j_k \forall (j,k) \in \mathcal{I}_3} \quad \sum_{i=1}^{N} \omega_i J_i(\mathcal{X}_i, \mathcal{U}_i), \tag{10a}$$

subject to:

$$(9), \qquad \forall\, (j, k+1) \in \mathcal{I}_3, \tag{10b}$$

$$\boldsymbol{g}(\boldsymbol{x}^j_{k+1}, \boldsymbol{u}^j_k) \leq 0, \qquad \forall\, (j, k+1) \in \mathcal{I}_3, \tag{10c}$$

$$\boldsymbol{u}^j_k = \boldsymbol{u}^l_k \text{ if } \begin{bmatrix} \boldsymbol{x}^{p(j)}_k \\ \hat{\boldsymbol{e}}^{p(j)}_k \end{bmatrix} = \begin{bmatrix} \boldsymbol{x}^{p(l)}_k \\ \hat{\boldsymbol{e}}^{p(l)}_k \end{bmatrix}, \ \forall\, (j,k), (l,k) \in \mathcal{I}_3, \tag{10d}$$

where $\mathcal{I}_3$ represents the set of indices (j,k) that occur in the scenario tree, N represents the number of scenarios, $\mathcal{X}_i$ and $\mathcal{U}_i$ represent the states and the control input that belongs to the i^{th} scenario in the tree and ω_i denotes the weight of the cost (J_i) associated with each scenario, with

$$J_i(\mathcal{X}_i, \mathcal{U}_i) = \sum_{k=0}^{N_p - 1} L(\boldsymbol{x}^j_{k+1}, \boldsymbol{u}^j_k), \ \forall \boldsymbol{x}^j_{k+1} \in \mathcal{X}_i, \boldsymbol{u}^j_k \in \mathcal{U}_i, \tag{11}$$

where $L(\boldsymbol{x}^j_{k+1}, \boldsymbol{u}^j_k)$ is the stage cost, N_p represents the length of the prediction horizon. The additional constraint that has to be satisfied at each node in the scenario tree is given by (10c). It enforces that the controller cannot anticipate the future realization of the uncertainty while computing its control moves (i.e. the control input for the branches originating from the same node must be the same, e.g. in Fig. 2, $\boldsymbol{u}^1_0 = \boldsymbol{u}^2_0 = \boldsymbol{u}^3_0$), this is enforced by (10d).

3.1 *Proposed model-error model update scheme*

Whenever new measurement information from the plant becomes available, the bound on the induced l_∞ gain of the unknown system can be computed from the sequence of inputs and outputs as in (Ljung, 2001):

$$\phi^s_k = \left[\hat{e}^s_k, \ \cdots, \ \hat{e}^s_{k-m} 6\right], \mu^s_k = \max_k \frac{|e^s_k|}{\|\phi^s_k\|_\infty}, \ \forall s \in \mathcal{I}_1, \tag{12a}$$

$$\gamma^s_k = \sqrt{m} \mu^s_k, \qquad \forall s \in \mathcal{I}_1, \tag{12b}$$

where m is the number of inputs ($\hat{e}_k^s$) that influence the output of the nonlinear operator (δ_k^s). Since we consider a static nonlinear operator, m is set to 1. If γ_k^s is larger than for some $s \in \mathcal{I}_1$, then the observed measurements cannot be obtained using the nominal model and the MEM such that $\|\delta_k^s\|_{i\infty} \leq 1$. Hence, the MEM is invalidated (Poolla et al., 1994). It was proposed in Thangavel et al. (2018c, 2019) to update the gain of the linear model (B^e) present in the MEM such that the updated MEM can describe the observed discrepancy between the projected plant measurements and the predicted model states. Adjusting only the gain of the linear model in the MEM over-approximates the uncertainty region described by the MEM and results in a performance loss. This can be avoided by updating the linear model (both A^e and B^e) present in the MEM using the online data. The two major factors to be considered while building the new MEM using the online data are:

(1) Existence of a sufficient level of excitation in the inputs obtained from the online data is necessary to recompute the model-error model;
(2) The information provided by the old MEM built using the offline data should be taken into account.

The condition to check the presence of persistent excitation signals of order n (number of unknown parameters to be estimated) in the input ($u_{[i]}$) is given by (Ljung, 1999)

$$\begin{bmatrix} \mathbb{R}_{u_{[i]}}(0) & \cdots & \mathbb{R}_{u_{[i]}}(n-1) \\ \vdots & \ddots & \vdots \\ \mathbb{R}_{u_{[i]}}(n-1) & \cdots & \mathbb{R}_{u_{[i]}}(0) \end{bmatrix} > 0, \tag{13}$$

where $\mathbb{R}_{u_{[i]}}(t) := \frac{1}{N_o-1}\sum_{j=1}^{N_o-1} u_{j,[i]}u_{j+t,[i]}$ and N_o represents the number of measurements available from the current plant run (online data). The condition (13) must be satisfied to update the MEM using the online data. In addition to this, the updated MEM should take into account the information provided by the MEM built using the offline data i.e. the uncertainty region described by the MEM built using the offline data should be contained within the uncertainty region described by the updated MEM at all frequencies. This can be enforced using

$$|H_{0,[j,i]}(e^{\bar{i}\omega t_s})| \leq |\tilde{H}_{[j,i]}(e^{\bar{i}\omega t_s})|, \forall \omega \leq \omega_n, i \in \mathcal{I}_4, j \in \mathcal{I}_1, \tag{14}$$

where $\mathcal{I}_4 = \{1, \cdots n_u\}$, t_s is the plant sampling time and ω_n is the Nyquist frequency. $\boldsymbol{H}_0(z)$ and $\tilde{\boldsymbol{H}}(z)$ represent the transfer function of the linear model present in the MEM obtained using the offline and online data and are given by $(z\boldsymbol{I} - \boldsymbol{A_0^e})^{-1}\boldsymbol{B_0^e}$ and $(z\boldsymbol{I} - \tilde{\boldsymbol{A}}^{\boldsymbol{e}})^{-1}\tilde{\boldsymbol{B}}^{\boldsymbol{e}}$. z is a delay block and $\boldsymbol{I}$ is an identity matrix. If $\boldsymbol{A_0^e}$ and $\tilde{\boldsymbol{A}}^{\boldsymbol{e}}$ are restricted to a diagonal matrix then $H_{0,[j,i]}$ and $\tilde{H}_{[j,i]}$ are given as

$$H_{0,[j,i]} = \frac{B^e_{0,[j,i]}}{z - A^e_{0,[j,j]}}, \quad \tilde{H}_{[j,i]} = \frac{\tilde{B}^e_{[j,i]}}{z - \tilde{A}^e_{[j,j]}}. \tag{15}$$

Substituting $|H_{0,[j,i]}|$ and $|\tilde{H}_{[j,i]}|$ in (14), we get

$$\sqrt{\frac{(B^e_{0,[j,i]})^2}{(cos(\omega t_s) - A^e_{0,[j,j]})^2 + sin(\omega t_s)^2}} \leq \sqrt{\frac{(\tilde{B}^e_{[j,i]})^2}{(cos(\omega t_s) - \tilde{A}^e_{[j,j]})^2 + sin(\omega t_s)^2}}. \tag{16}$$

Taking squares on both sides, applying trigonometric reductions and rearranging we get

$$\begin{matrix} (B^e_{0,[j,i]})^2((\tilde{A}^e_{[j,j]})^2+1) \\ -(\tilde{B}^e_{[j,i]})^2((A^e_{0,[j,j]})^2+1) \end{matrix} \leq \begin{matrix} 2(\tilde{A}^e_{[j,j]}(B^e_{0,[j,i]})^2 - \\ A^e_{0,[j,j]}(\tilde{B}^e_{[j,i]})^2)cos(\omega t_s). \end{matrix} \tag{17}$$

$cos(\omega t_s)$ can take values between ± 1. The following conditions ensures (14) is satisfied at all frequencies provided $\boldsymbol{A_0^e}$ and $\tilde{\boldsymbol{A}}^{\boldsymbol{e}}$ are diagonal matrices:

$$\begin{matrix} (B^e_{0,[j,i]})^2((\tilde{A}^e_{[j,j]})^2+1) \\ -(\tilde{B}^e_{[j,i]})^2((A^e_{0,[j,j]})^2+1) \end{matrix} \leq \begin{matrix} \pm 2(\tilde{A}^e_{[j,j]}(B^e_{0,[j,i]})^2 - \\ A^e_{0,[j,j]}(\tilde{B}^e_{[j,i]})^2). \end{matrix} \tag{18}$$

The formulation of the optimization problem that is solved to update the MEM if the MEM obtained using the offline data is invalidated is given as

$$\min_{\tilde{\boldsymbol{A}}^{\boldsymbol{e}}_{N_o}, \tilde{\boldsymbol{B}}^{\tilde{e}}_{N_o}} \frac{1-\alpha}{N_o} O_1 + \frac{\alpha}{N_o} O_2 \tag{19a}$$

subject to

$$\breve{\boldsymbol{e}}_0 = \mathbb{P}(\boldsymbol{z}_0) - \boldsymbol{x}_0, \quad \breve{\boldsymbol{e}}_{k+1} = \boldsymbol{A_0^e}\breve{\boldsymbol{e}}_k + \boldsymbol{B_0^e}\boldsymbol{u}_k, \quad \forall k \in \mathcal{I}_5, \tag{19b}$$

$$\hat{\boldsymbol{e}}_{k+1} = \tilde{\boldsymbol{A}}^{\boldsymbol{e}}_{N_o}\hat{\boldsymbol{e}}_k + \boldsymbol{B}^{\boldsymbol{e}}_{N_o}\boldsymbol{u}_k, \quad \forall k \in \mathcal{I}_5, \tag{19c}$$

$$\hat{\boldsymbol{e}}_0 = \mathbb{P}(\boldsymbol{z}_0) - \boldsymbol{x}_0, \quad -1 \leq \mathrm{diag}(\boldsymbol{A}^{\boldsymbol{e}}_{N_o}) \leq 1, \tag{19d}$$

$$-\hat{\boldsymbol{e}}_{k+1} \leq \boldsymbol{e}_{k+1} \pm \boldsymbol{\sigma}_{k+1} \leq \hat{\boldsymbol{e}}_{k+1}, \forall k \in \mathcal{I}_5, \tag{19e}$$

$$(18), \quad \forall j \in \mathcal{I}_1, i \in \mathcal{I}_4, \tag{19f}$$

where $\mathcal{I}_5 := \{0, \cdots, N_o - 1\}$, and $\boldsymbol{A}^{\boldsymbol{e}}_{N_o} \in \mathbb{R}^{n_x \times n_x}$, $\boldsymbol{B}^{\boldsymbol{e}}_{N_o} \in \mathbb{R}^{n_x \times n_u}$ describe the dynamics of the linear model in the MEM obtained using the online data. $\breve{\boldsymbol{e}}_k$ represents the prediction of the linear model in the MEM that was obtained using offline data. The objective function (19a) is chosen to minimize the difference between the uncertainty region described by the MEM built using the offline data and the one built using the online data (given by O_1), and the uncertainty region around the nominal model of the plant which encloses the observed online data (given by O_2), where O_1 and O_2 are defined as

$$O_1 = \sum_{k=0}^{N_o-1}(\hat{\boldsymbol{e}}_{k+1} - \breve{\boldsymbol{e}}_{k+1})^T\boldsymbol{Q}(\hat{\boldsymbol{e}}_{k+1} - \breve{\boldsymbol{e}}_{k+1}) \tag{20}$$

$$O_2 = \sum_{k=0}^{N_o-1}\hat{\boldsymbol{e}}_{k+1}^T\boldsymbol{Q}\hat{\boldsymbol{e}}_{k+1} \tag{21}$$

α is a tuning parameter and is chosen between 0 and 1. If α is chosen close to 0 more emphasis is given to the offline data and if it is chosen close to 1 more emphasis is given to the online data. The constraints (19c)-(19e) are similar to the constraints (5b) and (6). In the absence of measurement noise, $\boldsymbol{\sigma}_{k+1}$ is set to 0. The constraint (19f) ensures that the updated MEM along with the nominal model describes all the plant measurements recorded in the offline data.

3.2 Algorithm

The algorithm for the implementation of the proposed robust multi-stage NMPC with MEM is given below.

- Step 1: Model-error model is obtained by solving (5) using the offline data.
- Step 2: Set $\boldsymbol{A^e} = \boldsymbol{A_0^e}$, $\boldsymbol{B^e} = \boldsymbol{B_0^e}$ in (10).
- Step 3: Solve (10) and apply the first control input to the plant.
- Step 4: After a new measurement has been received, compute γ_k^s using (12) with $\boldsymbol{A^e} = \boldsymbol{A_0^e}, \boldsymbol{B^e} = \boldsymbol{B_0^e}$.
- Step 5: **If** (13) is not satisfied & $\gamma_k^s \nleq 1 \forall s \in \mathcal{I}_1$:
  Adjust the gain of the linear model present in MEM as in (Thangavel et al., 2018c). Set $\boldsymbol{A^e} = \boldsymbol{A_0^e}$, $\boldsymbol{B^e} = \boldsymbol{B^e_{N_m}}$.
  Else if (13) is satisfied & $\gamma_k^s \nleq 1 \forall s \in \mathcal{I}_1$:
  Update the MEM by solving (19). Set $\boldsymbol{A^e} = \tilde{\boldsymbol{A}}^{\boldsymbol{e}}_{N_o}$, $\boldsymbol{B^e} = \tilde{\boldsymbol{B}}^{\boldsymbol{e}}_{N_o}$.

Else: Continue

Step 6: **If:** End time is reached *Stop*

Else: Reinitialize the robust NMPC with the plant measurements. Go to Step 3.

4. CASE STUDY

We consider the nonlinear continuous stirred tank reactor (CSTR) benchmark problem from Klatt and Engell (1998) to show the advantages of multi-stage NMPC with model-error model using the proposed model-error model update strategy (abbreviated as MS-MEM-MU) over the previous approach using only gain updates presented in Thangavel et al. (2018c) (is abbreviated as MS-MEM-GU). The true plant model along with the nominal model of the plant can be obtained from Thangavel et al. (2018c).

The sampling time was chosen as 0.005 h (18 s). The nonlinear dynamics were discretized using orthogonal collocation on finite elements and the optimization problems were solved using IPOPT (Wächter and Biegler, 2006). The first and second order derivative information to IPOPT were provided by CasADi (Andersson et al., 2019). The objective is to maximize the number of moles of product B produced per hour ($\dot{n}_{\rm B} = \dot{V}_{\rm in}c_{\rm B}$) while respecting the constraint on the reactor temperature ($T_R \leq 142$). This can be achieved by increasing the concentration of product B and the feed rate F. The length of the prediction horizon and of the robust horizon of the NMPC are chosen as $N_p = 5$ and $N_r = 1$. The recursive feasibility, stability and constraint satisfaction of the MS-MEM NMPC were verified using simulation studies. The bound ($\boldsymbol{\sigma}$) on the measurement noise is given by $[0.005, 0.005, 0.05]$. The data obtained when the plant is controlled using a standard NMPC with nominal model for 0.25 h (15 minutes) is considered as the offline data. The initial model-error model used in multi-stage NMPC with MEM is built by solving the optimization problem (5) using the offline data. The order of the excitation signal n is 2, since the structure of $\boldsymbol{A}^e$ is restricted to a diagonal matrix. The tuning parameter (Λ) is chosen as $[2,\, 2,\, 2]^T$. The constraint on the reactor temperature is implemented as a soft constraint to prevent the NMPC optimization problem from becoming infeasible in case of constraint violations.

Fig. 3 shows the results that were obtained using different NMPC strategies in the presence of measurement noise. Standard NMPC with the nominal model violates the constraint because the nominal model does not include the exothermic reaction $B \rightarrow C$ that is taking place inside the reactor. The MS-MEM-GU and MS-MEM-MU NMPC approaches consider the influence of the unmodelled dynamics of the plant using a model-error model and are able to satisfy the constraints and to maximize the number of moles of product B produced. Fig. 4 shows the gain estimate of the unknown nonlinear static map of the MEM (γ_k^s) obtained from the plant measurements using (12), where the MEM is updated at each NMPC iteration if the observed measurements invalidate the MEM built using the offline data. It can be seen from figure, that γ^3 is greater than 1 at the first-time step. The MEM is invalidated at the first-time step and has to be updated. The condition (13) is not satisfied only at the first-time step hence only the gain of the linear model present in the MEM is updated after the first NMPC iteration and the MEM is obtained by solving (19) for all the subsequent NMPC iterations when using the MS-MEM-MU NMPC approach. Only the gain of the linear model present in the MEM is updated at all NMPC iterations when using the MS-MEM-GU approach. The estimate (γ_k^s) of the gain of the unknown mapping obtained using the updated model-error model is always less than the value of the chosen robust factor $\boldsymbol{\Lambda}$ as shown in Fig. 4. Fig. 5 shows the Bode magnitude plot of the linear model present in the updated MEM obtained at time 0.25 h when using the MS-MEM-GU and MS-MEM-MU NMPC approaches. The magnitude plot of the linear model corresponding to the state $c_{\rm A}$ is not plotted in the figure because γ^1 is always less than 1 as shown in Fig. 4, hence $H_{0,[1,1]}$ it is not updated. The model-error model obtained by solving (19) tightly approximates the uncertainty region around the nominal model based on the observed measurements at all frequencies when compared to updating only the gain of the linear model present in the MEM as shown in Fig. 5. This results in more moles of product B produced when using the proposed MS-MEM-MU NMPC approach when compared to the MS-MEM-GU NMPC approach.

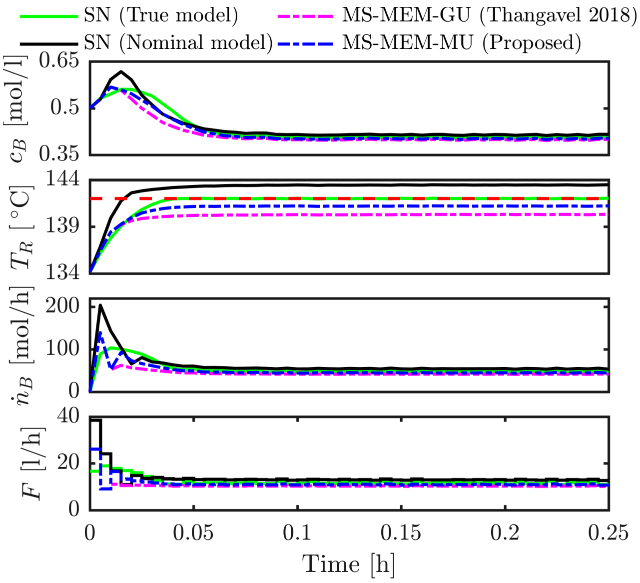

Fig. 3. Comparison of the results obtained using different NMPC strategies. SN - Standard NMPC.

Table 1. Consolidated results.

NMPC Strategies	$\sum n_{\rm B}$ [up to 0.25 h] No noise	Noise	CPU [s]
Standard NMPC (True Model)	13.44	13.44	0.12
Standard NMPC (Nominal Model)	CV	CV	0.13
MS-MEM-GU (Thangavel et al., 2018c)	11.79	11.28	1.95
MS-MEM-MU (Proposed)	12.68	12.37	2.02

CV - Constraint Violation

Table 1 shows the number of moles of product B produced until 0.25 h using the different NMPC strategies along with their corresponding computation times, where CV denotes constraint violation. Standard NMPC with the nominal model produces more moles of product B when compared to the other NMPC strategies but it violates the constraints. There is a 10% increase in the number of moles of product B produced when using the MS-MEM-MU NMPC approach over the MS-MEM-GU NMPC ap-

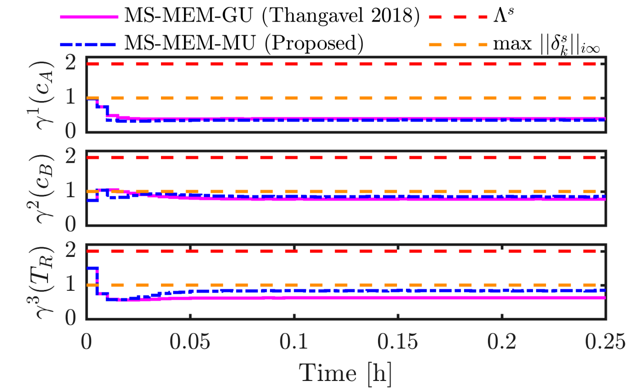

Fig. 4. Gain estimate (γ_k^s) of the unknown mapping (δ_k^s). - - - Robust factor (Λ). - - - Upper bound on the gain of the unknown mapping of the MEM as in (4).

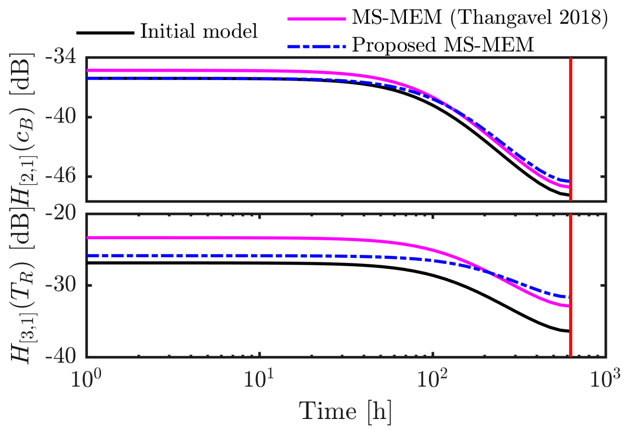

Fig. 5. Bode magnitude plots of the linear models present in the updated MEM obtained at time 0.25 h.

proach. MS-MEM NMPC approaches perform better in the absence of measurement error because a zero value of σ considered in the optimization problem (5) decreases the uncertainty region associated with the nominal model due to the presence of accurate plant measurements. The time taken to solve the proposed MS-MEM-MU NMPC approach is slightly higher than the MS-MEM-GU NMPC approach, because the MEM is obtained by solving an optimization problem if the MEM is invalidated at an NMPC iteration in the former approach whereas the gain of the linear model present in the MEM can be updated using matrix multiplication in MS-MEM-MU approach which is computationally less expensive.

5. CONCLUSION

A new scheme to update the model-error model used in multi-stage NMPC with model-error model if the observed plant measurement invalidates the MEM is presented. The proposed scheme tightly approximates the uncertainty region around the nominal model of the plant at all frequencies and results in a better performance when compared to the previous approach (Thangavel et al., 2018c). Our future work will focus on extending the proposed approach to work in a moving window fashion to tackle the increase of the computational complexity of the proposed model-error model update approach with the increase in the number of measurements.

REFERENCES

Andersson, J.A.E., Gillis, J., Horn, G., Rawlings, J.B., and Diehl, M. (2019). CasADi – A software framework for nonlinear optimization and optimal control. *Mathematical Programming Computation*, 11(1), 1–36.

Campo, P. and Morari, M. (1987). Robust model predictive control. In *Proc. of the American Control Conference*, 1021–1026.

Falugi, P. and Mayne, D.Q. (2014). Getting robustness against unstructured uncertainty: A tube-based mpc approach. *IEEE T AUTOMAT CONTR*, 59(5), 1290–1295.

Klatt, K.U. and Engell, S. (1998). Gain-scheduling trajectory control of a continuous stirred tank reactor. *Computers & Chemical Engineering*, 22(4), 491 – 502.

Ljung, L. (ed.) (1999). *System Identification (2nd Ed.): Theory for the User*. Prentice Hall PTR, Upper Saddle River, NJ, USA.

Ljung, L. (2001). Estimating linear time-invariant models of nonlinear time-varying systems. *Eur J Control*, 7(2), 203 – 219.

Lucia, S., Finkler, T., Basak, D., and Engell, S. (2012). A new robust nmpc scheme and its application to a semi-batch reactor example. *IFAC-PapersOnLine*, 45(15), 69 – 74.

Lucia, S., Finkler, T., and Engell, S. (2013). Multi-stage nonlinear model predictive control applied to a semi-batch polymerization reactor under uncertainty. *J Process Contr*, 23, 1306–1319.

Mayne, D.Q. (2014). Model predictive control: Recent developments and future promise. *Automatica*, 50(12), 2967 – 2986.

Mayne, D., Seron, M., and Rakovic, S. (2005). Robust model predictive control of constrained linear systems with bounded disturbances. *Automatica*, 41, 219 – 224.

Poolla, K., Khargonekar, P., Tikku, A., Krause, J., and Nagpal, K. (1994). A time-domain approach to model validation. *IEEE Transactions on Automatic Control*, 39(5), 951–959.

Schoukens, J., Vaes, M., and Pintelon, R. (2016). Linear system identification in a nonlinear setting: Nonparametric analysis of the nonlinear distortions and their impact on the best linear approximation. *IEEE Control Systems Magazine*, 36(3), 38–69.

Scokaert, P. and Mayne, D. (1998). Min-max feedback model predictive control for constrained linear systems. *IEEE T AUTOMAT CONTR*, 43(8), 1136–1142.

Subramanian, S., Lucia, S., and Engell, S. (2015). Handling structural plant-model mismatch via multi-stage nonlinear model predictive control. In *European Control Conference 2015*, 1602–1607.

Thangavel, S., Lucia, S., Paulen, R., and Engell, S. (2018a). Dual robust nonlinear model predictive control: A multi-stage approach. *Journal of Process Control*, 72, 39 – 51.

Thangavel, S., Aboelnour, M., Lucia, S., Paulen, R., and Engell, S. (2018b). Robust dual multi-stage nmpc using guaranteed parameter estimation. *IFAC-PapersOnLine*, 51(20), 72 – 77.

Thangavel, S., Paulen, R., and Engell, S. (2020). Adaptive multi-stage NMPC using sigma point principles. *2020 19th European Control Conference (ECC)*.

Thangavel, S., Subramanian, S., and Engell, S. (2019). Robust nmpc using a model-error model with additive bounds to handle structural plant-model mismatch. *IFAC-PapersOnLine*, 52(1), 592 – 597.

Thangavel, S., Subramanian, S., Lucia, S., and Engell, S. (2018c). Handling structural plant-model mismatch using a model-error model in the multi-stage NMPC framework. *IFAC-PapersOnLine*, 51(15), 1074 – 1079.

Wächter, A. and Biegler, L. (2006). On the implementation of a primal-dual interior point filter line search algorithm for large-scale nonlinear programming. *Math Program*, 106, 25–57.